SKB

TECHNICAL REPORT 91-61

Heat propagation from a radioactive waste repository. SKB 91 reference canister

R Thunvik, C Braester

Royal Institute of Technology, Stockholm, Sweden

March 1991

SVENSK KÄRNBRÄNSLEHANTERING AB
SWEDISH NUCLEAR FUEL AND WASTE MANAGEMENT CO

BOX 5864 S-102 48 STOCKHOLM

TEL 08-665 28 00 TELEX 13108 SKB S
TELEFAX 08-661 57 19

HEAT PROPAGATION FROM A RADIOACTIVE WASTE REPOSITORY. SKB 91 REFERENCE CANISTER

Roger Thunvik, Carol Braester

Royal Institute of Technology, Stockholm, Sweden

March 1991

HEAT PROPAGATION FROM A RADIOACTIVE WASTE REPOSITORY

SKB 91 Reference Canister

Roger Thunvik
Carol Braester

Royal Institute of Technology
Stockholm, Sweden

March 1991

ABSTRACT

A study of heat propagation around a hypothetical radioactive waste repository is presented. The investigated flow domain was limited to a quarter of the flow domain around a single canister due to symmetry by vertical planes passing through the centre of the canister, half distance between the adjacent tunnels and the adjacent canisters. Strictly speaking, such an approach is applicable to a repository of infinite extent. However, from a practical point of view this assumption applies to all canisters but the ones close to the edge of the repository. The following different material regions were considered: (i) Canister containing the spent fuel, (ii) Buffer (bentonite) around the canister, (iii) Backfilled (mixture of bentonite and sand) tunnels, and (iv) host Rock. The canister material was represented by a "homogenized" medium obtained by weighted averaging of the main constituents of the canister, viz. spent fuel, copper and lead. A geothermal gradient of 13 °C/km was assumed. The initial heat effect per canister was 1066 W. The total vertical extent of the flow domain considered was about 1500 metres. The base case, with 6.2 m canister spacing and 30 m tunnel spacing, resulted in a maximum temperature at the canister/buffer interface of about 66 °C (corresponding to a temperature rise of about 54 °C), and about 50 °C (about 38 °C temperature rise) in the rock.

CONTENTS

List of symbols

C	heat capacity
e^n	normal component of the heat flux at the boundary
h	height of canister
l_b	equivalent borehole side ($l_b = \frac{\sqrt{\pi}}{2} r_b$)
l_c	equivalent canister side ($l_c = \frac{\sqrt{\pi}}{2} r_c$)
l_x	the length of the investigated domain in the x-direction (= tunnel spacing/2)
l_y	the length of the investigated domain in the y-direction (= canister spacing/2)
l_z	the length of the investigated domain in the z-direction
q	thermal flux
Q	source/sink in the energy conservation equation
Q_o	initial strength of the heat source function
r_c	canister radius
r_b	borehole radius
t	time
Δt	time interval
T	temperature
x	Cartesian coordinate in the horizontal plane
y	Cartesian coordinate in the horizontal plane
z	Cartesian coordinate in the vertical direction
t	time

Greek

$\alpha_1, \alpha_2, \alpha_3$	coefficients in the heat source function
λ	thermal conductivity
ρ	density
Ψ	basis function

Subscripts

b	borehole
c	canister
i,j	indices for Cartesian tensor notation; repeated indices indicate summation over these indices (i,j = 1,2,3)
,i	spatial derivative (i = 1,2,3)
,t	partial time derivative

Superscripts

I,J,K -	node indices, repeated indices indicate summation over these indices (I,J,K =1,2,...N, where N is the number of nodal points

1. INTRODUCTION

The present investigation is carried out in the course of the analysis of the thermal effects due to hypothetical radioactive waste repository sites, on the surrounding environment. The heat released by the radioactive waste will increase the temperature of the surrounding buffer material and rock. This study investigates the temperature distribution around the canisters for the basic geometrical setting as well as the effect of varying the distance between the adjacent boreholes for the location of the canister and the distance between adjacent tunnels.

Due to the nonlinearity and coupling between the flow and heat model equations, the complicated geometry of the investigated domains, and inhomogeneity in rock properties, including fractured zones, the calculations are to be carried out by a numerical method of solution.

Prior to the analysis of various prospective radioactive sites, it is necessary to study the relevance of the different flow phenomena and of the local inhomogeneities in the rock properties, on the studied phenomenon. Disregarding irrelevant flow phenomena may lead to a significant decrease in the effort for data preprocessing, to the decrease of the computational effort and of the needed resources, and to the increase in the accuracy of the results. A careful analysis of the significance of the different parameters and phenomena is required before deciding which effects should be disregarded, and conduct calculations under simplifying assumptions. In the frame of such possible simplifications we analyzed if the local inhomogeneity in the material properties due to the buffer has any significant effect on the maximum reached temperatures in comparison with the case where we attributed rock properties to the whole domain.

The present analysis is carried out under the assumption that heat is transferred to the surrounding only by conduction. It should be pointed out that this assumption is conservative, since possible convection currents will have a cooling effect. The analysis of the conditions under which convection currents occur, as a result of the thermal conditions prevailing in the surrounding of the repository, will be the subject of a another study.

The investigated domain is limited by vertical planes passing through the centre of the canister, half distance between the adjacent caverns and the adjacent canisters. For reasons of symmetry, these vertical planes are no heat flow boundaries or insulated boundaries. This implies that the calculations for the considered flow domain, confined within vertical planes of insulated boundaries, account for the effect of all the canisters contained within the repository.

Strictly speaking this assumption applies to a repository of infinite extent. Practically, it applies to all canisters but the ones close to edge of the repository (where the assumed symmetry does apply). Obviously, the maximum temperature reached at the location of the canisters close to the boundaries will be smaller than at the locations far from the boundaries, for which the calculations are performed.

2. PROBLEM DESCRIPTION

A KBS-3 type of repository (Figure 1) is assumed to consist of a series of parallel tunnels, located at a depth of 500 metres below the rock surface. The distance between the longitudinal axes of the adjacent tunnels is 30 meters. The characteristic basic setting considered is: Dimensions of tunnel cross-section 4.5 metres height and 3.7 metres width, and canisters (Figure 2) containing the spent fuel and lead disposed in boreholes along the tunnels at a distance between the axes of adjacent boreholes of 6.2 metres.

The length of a borehole is 7.7 metres below the tunnel bottom, and the borehole diameter is 1.5 metres. The canisters, of 0.8 metres diameter, are disposed at a depth of 7.5 metres below the bottom of the tunnel. After the emplacement of the canisters, the tunnels are filled with a backfill material, consisting of a mixture of sand and bentonite. The canisters, made of copper and filled with lead and spent fuel, are surrounded by bentonite.

The area over which a typical repository spreads is a rectangle with a side of one kilometre. As already mentioned for reasons of symmetry it is enough to study the domain presented in Figure 3, representing a quarter of the flow domain around a canister.

The investigated domain extends to a depth of 1000 metres below the level of the repository. The region below this depth is assumed to be insignificantly affected by the thermal conditions prevailing in the region of the repository.

The top (surface ABCD in Figure 3), and the bottom of the investigated domain (EFGH surface Figure 3), were considered constant temperature boundaries and set according to the geothermal conditions at the Finnsjön study site (Ahlbom and Tirén [1989]). For reasons of symmetry, the lateral sides boundaries of the domain, i.e. ABFE, BCGF, DCGH and ADHE were considered insulated boundaries.

For convenience the circular cross-section of the canister was approximated by a square with the sides such that the equivalent

(orthorhombic) canister volume becomes the same as for the actual (cylindrical) canisters. The cross section of the tunnel was approximated by a rectangle. The studied problem is the temperature distribution in time in the studied domain, as a result of the time dependent heat output due to the decaying radioactive material.

The purpose of this investigation may be summarized as follows:

(I) To study the temperature distribution for the basic geometrical setting (Figure 1) and considering the actual properties of the materials in place.

(II) To study the temperature distribution for reduced distances between the canisters and between the tunnels.

(III) To find a geometrical configuration corresponding to a maximum temperature of 100 °C at the interface between the canister and the bentonite buffer.

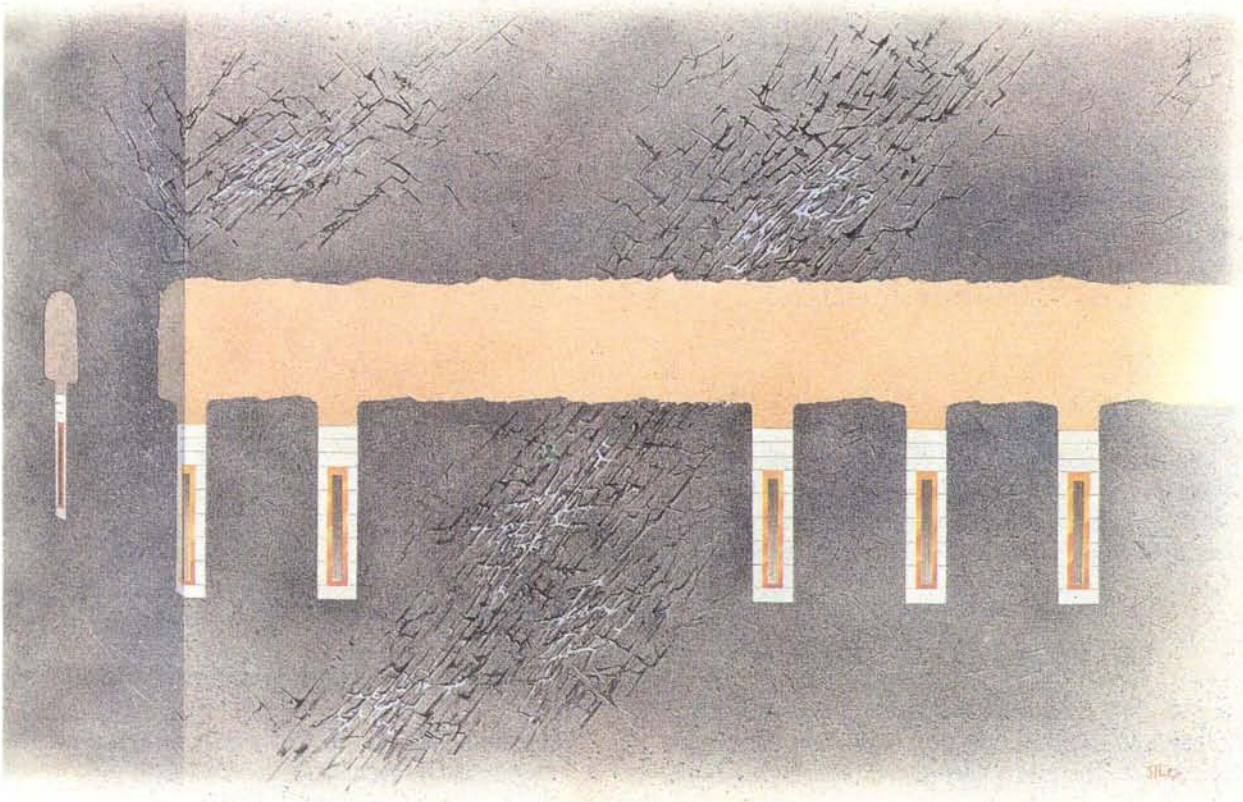

Figure 1. KBS-3 type of repository.

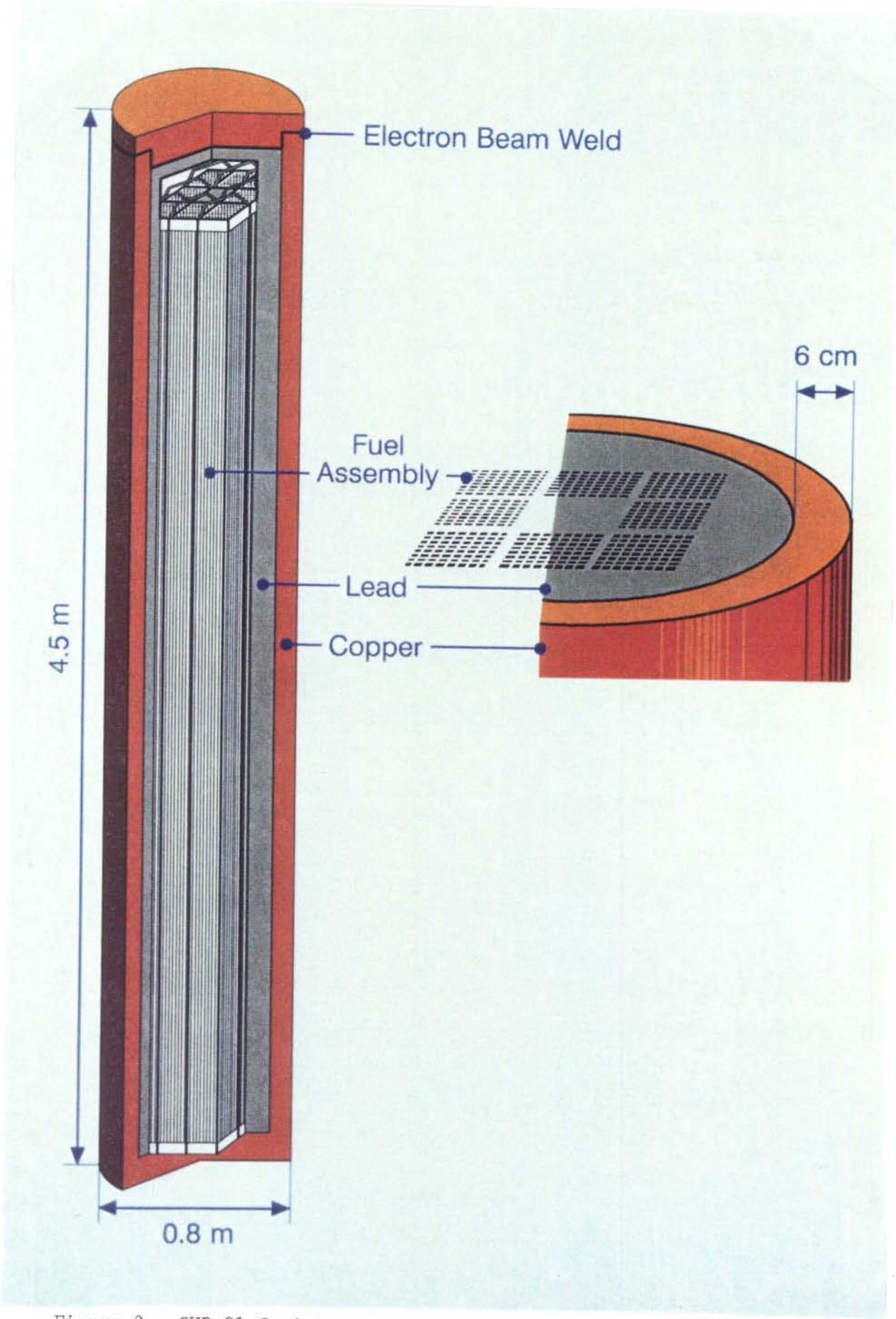

Figure 2. SKB 91 Canister.

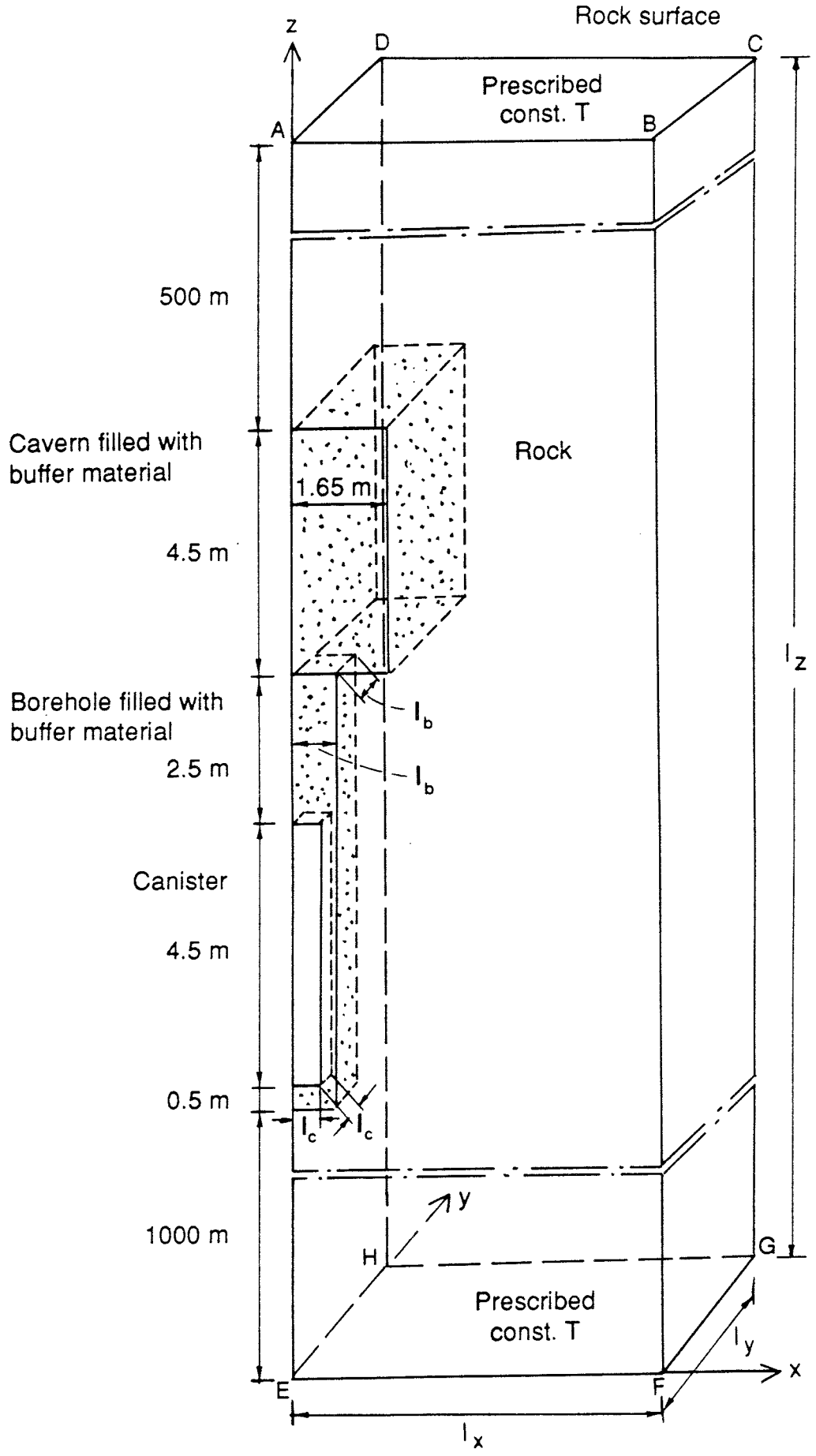

Figure 3. Schematic representation of the flow domain (l_c = 0.3545 m, l_b = 0.6647m).

3. MODEL EQUATIONS

Heat conduction is governed by the following equations:

The heat flux equation (Fourier's law)

$$q_i = - \lambda T_{,i} \tag{1}$$

where q_i is the thermal flux in the i direction, λ denotes the thermal conductivity, and T is temperature.

The thermal energy conservation equation

$$(\rho C T)_{,t} + q_{i,i} + Q(t) = 0 \tag{2}$$

Substitution of (1) into (2) yields

$$(\rho C T)_{,t} - (\lambda T_{,i})_{,i} + Q(t) = 0 \tag{3}$$

where ρ the density, C is the specific heat, $T = T(x,y,z,t)$ is the temperature, λ is the thermal conductivity and $Q(t)$ represents the time dependent heat source.

Boundary and initial conditions

The boundary conditions are

$$\begin{aligned}
&0 < x < l_x \; ; \; 0 < y < l_y \; ; \; z = 0 : T = T_{bottom} \\
&0 < x < l_x \; ; \; 0 < y < l_y \; ; \; z = l_z : T = T_{surf} \\
&x = 0 \; ; \; 0 < y < l_y \; ; \; 0 < z < l_z : q_{,x} = 0 \\
&x = l_x \; ; \; 0 < y < l_y \; ; \; 0 < z < l_z : q_{,x} = 0 \\
&y = 0 \; ; \; 0 < x < l_x \; ; \; 0 < z < l_z : q_{,y} = 0 \\
&y = l_y \; ; \; 0 < x < l_x \; ; \; 0 < z < l_z : q_{,y} = 0
\end{aligned} \tag{4}$$

where l_x, l_y and l_z are the dimensions of the domain in the x, y, and z directions, respectively, and T_{surf} denotes the prescribed temperature on top of the rock surface and T_{bottom} denotes the prescribed temperature on the bottom of the flow domain, respectively.

The initial condition considered was a reference temperature assumed to follow the geothermal gradient. A distributed heat source ($Q(t)$) corresponding to the variation in time of the thermal energy released from the radioactive waste is applied at the canister location.

4. NUMERICAL CALCULATIONS

The geometrical configuration of the considered domain, a quarter of the domain around the canister, is presented in Figure 3. The different materials in the domain are: (i) Granite host rock, (ii) Buffer material consisting of a mixture of sand and bentonite back-filling the tunnels, (iii) Bentonite surrounding the canisters and (iv) Canisters, consisting of copper and lead, containing the spent fuel. The thermal properties of the different materials considered in the domain are given in Table I below.

TABLE I. Thermal properties of the flow domain for the SKB 91 Canister

Parameter	Canister	Buffer[1)]	Tunnel	Rock
Density ρ [kgm^{-3}]	5600	2000	2100	2700
Spec. heat capacity C [$J\ kg^{-1}\ K^{-1}$]	390	1100	1400	800
Thermal conductivity λ [$Wm^{-1}\ K^{-1}$]	390	0.75	2.4	3.0
Heat effect/canister Q_{tot} [W]	1066[2)]			
Volumetric heat effect Q_o [Wm^{-3}]	471.26[2)]			

[1)] The values correspond to dry conditions.

[2)] Initial heat effect at the emplacement of the canister.

The thermal properties of the "equivalent copper canister", here called the SKB 91 Canister, are based on the material composition of the major constituents (i.e. spent fuel, copper and lead) of the canister (Bergström [1990], Kjellbert [1990] as given in Table II in the sequel.

The time dependent variation of the heat generation per canister during the first 1000 years of deposition, is approximated by a function of the following type:

$$Q(t)/Q_o = (\alpha_1 e^{-\alpha_2 t} + (1-\alpha_1) e^{-\alpha_3 t})$$

where $Q(t)$ denotes the time dependent heat effect, Q_o denotes the heat effect at the time of the deposition, t is time, α_1, α_2 and α_3 are constant coefficients. These are determined by minimizing a function for the sum of the squares of the differences between the heat function values and the observed values. The coefficient values are given in Table III.

Graphical representations of the variation of $Q(t)/Q_o$ in time, showing the discrete input data and the curves fitted using the above relationship, as well as the heat function parameter values used in the calculations are presented in Figure 4.

TABLE II. Thermal properties of the SKB 91 "Equivalent Copper Canister"

Weight kg	Material	Heat capacity J kg^{-1} K^{-1}	Heat capacity k J K^{-1}	Density kg m^{-3}
6585	Copper	390	2267	
14500	Lead	130	1885	
2000	Fuel	250	500	
12700	Copper equivalent canister	390	4955	5600

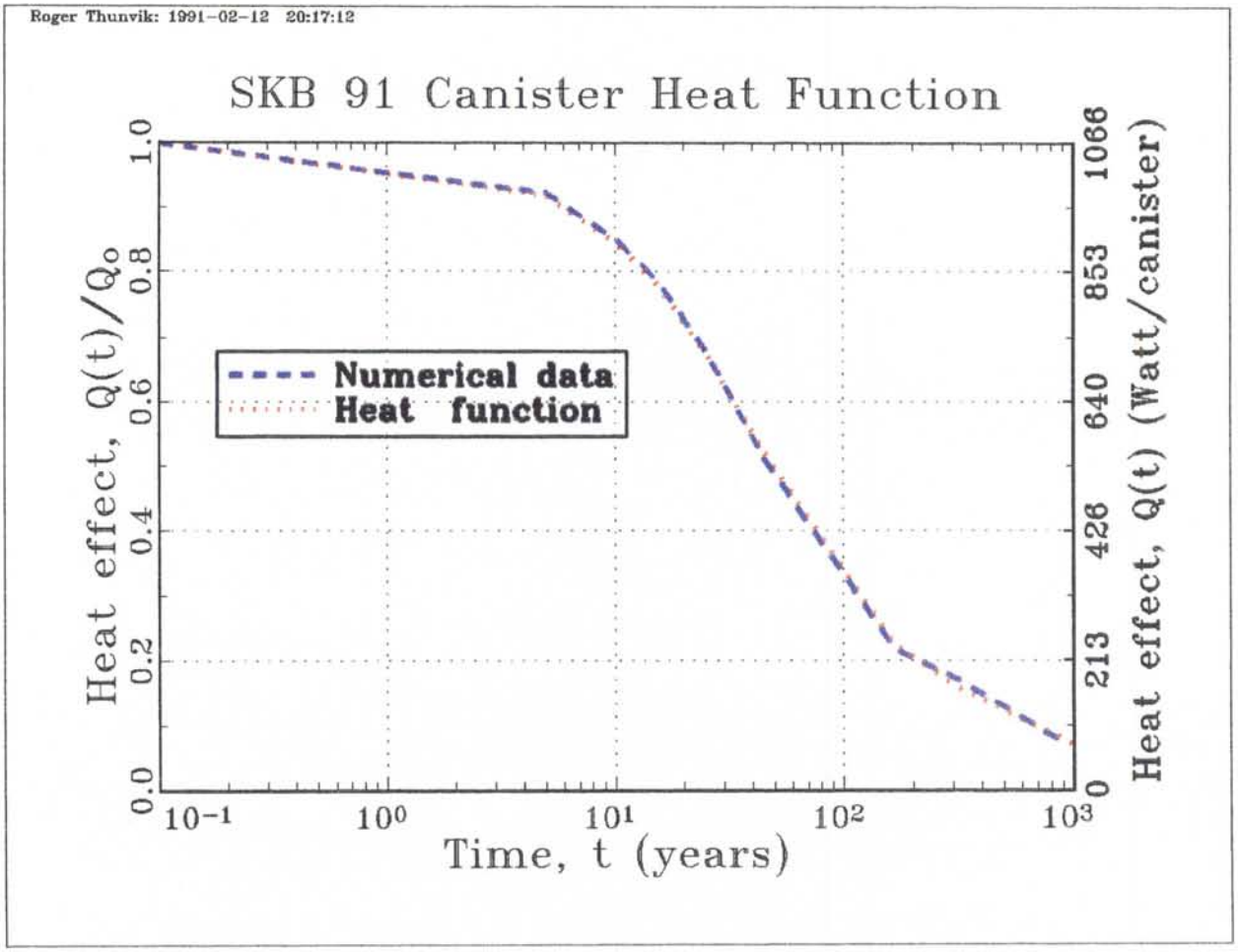

Figure 4. Time dependent heat function used for the SKB 91 Canister.

TABLE III. Heat source function parameter data:

Heat source function:[1]	
$Q(t)/Q_o = (\alpha_1 e^{-\alpha_2 t} + (1-\alpha_1) e^{-\alpha_3 t})$	
Parameter	Value
Q_{tot} [W]	1066
Q_o [W·m^{-3}]	471.26
α_1	$7.531212 \cdot 10^{-1}$
α_2	$2.176060 \cdot 10^{-2}$
α_3	$1.277985 \cdot 10^{-3}$

Geometric characteristics of the heat source (3-d Cartesian):			
$r_c = 0.4$ m ,	$l_c = \frac{\sqrt{\pi}}{2} r_c = 0.3545$ m		
$r_b = 0.75$ m ,	$l_b = \frac{\sqrt{\pi}}{2} r_b = 0.6647$ m		
$V = 4\, l_c^2\, h = 2.262$ m^3 ($h = 4.5$ m)			
$X_{min} =$	0 ,	$X_{max} =$	0.3545
$Y_{min} =$	0 ,	$Y_{max} =$	0.3545
$Z_{min} =$	1000.5 ,	$Z_{max} =$	1005.0

The geothermal gradient was here assumed to be 13 °C/km. The initial temperature at a depth of 500 m was assumed to be 12.3 °C and at the upper boundary the temperature was assumed to be 5.8 °C. The geothermal gradient is applied to the flow domain by prescribing constant temperature (T = 25.45 °C, Z = *0*) at the bottom boundary and (T = 5.8 °C, Z = *1512 m*) at the top boundary.

The present calculations were preceded by a set of calculations[2] in

[1] *t is time in years.*

[2] To be presented in a separate report.

order to check the influence of varying the material properties as well as the geometric configuration associated with the spacing of the tunnels as well as the canisters. In addition the effects of the discretization of the flow domain, interpolation order of the elements, and the time integrations were checked.

The flow domain was discretized by 210 quadratic (27-node hexahedron) three-dimensional elements and the total number of nodes was 2233. The time integration was performed according to a backward Euler (implicit) scheme for about 150 time steps. The time step was gradually increased with an initial time step in the range $5 \cdot 10^3$-$5 \cdot 10^4$ seconds and the calculations were carried out for a final time between 100 and 1000 years.

The results for each setting are displayed in the form of curves to show the temperature at relevant sections, such as between the tunnels, between the canisters and along the centre of the borehole. Two types of curves are considered, one which displays time dependent temperature curves for selected points on a horizontal plane perpendicular to the longitudinal centre line of the canister (X=0 , Y=0, 1000.5 < Z 1005.0) and the other temperature profiles along the x- , y- and z-directions for selected time levels.

The following naming convention was introduced to facilitate the identification of the graphical displays:

CBT1*n*HI1 : $0 < X < l_x$, $y = 0$, $Z = 1002.75$

CBT1*n*HI2 : $X = 0$, $0 < y < l_y$, $Z = 1002.75$

CBT1*n*HI3 : $X = 0$, $y = 0$, $990 < Z < 1020$

Canister : $0 < X < 0.3545$, $0 < y < 0.3545$, $1000.5 < Z < 1005$

where l_x is half the spacing between tunnels, l_y is half the spacing between the canisters and n denotes the case no ($n = a, b, \ldots, k$). The base case is illustrated by a perspective plot of the temperature contour lines approximately at the time when the maximum temperature was reached in the canister.

In the calculations the canister and the spent fuel were represented by a single equivalent "copper like" medium whose physical properties were obtained by taking the weighted averages of the specific heat of the

main constituents of the actual canister.

In addition to analyzing the heat propagation from the SKB 91 Canister for the base case, i.e. for a canister spacing of 6.2 m and a tunnel spacing of 30 m, the object was to find a geometric configuration leading to a maximum of 100 °C at the interface between the canister and the buffer.

The lateral extent of the flow domain subject to calculation was in the x-direction (l_x) between 10 and 15 m (corresponding to a spacing between the tunnels of 20 - 30 m) and in the y-direction ($l_{y)}$ between 1.5 and 3.1 m (corresponding to a spacing between the canisters along each tunnel of 3.0 - 6.2 m).

The physical properties of the flow domain, the thermal properties of the "equivalent" canister (SKB 91 Canister), and the heat source parameter data are presented in Tables I, II and III. The time dependent heat function is presented in Fig. 4.

SKB 91 Canister - Tunnel spacing=30 m

Two cases were carried out: The base case CBT1a (6.2x30m) and three cases with a reduced canister spacing CBT1i (5x30m), CBT1k (4x30m), and CBT1b (3.0x30m). The results of the calculations are summarized in Table IV. A graphical presentation of the results from the base case CBT1a can be found in Appendix I.

CBT1a (6.2x30m): This case is considered the base case (6.2 m canister spacing and 30 m tunnel spacing). The maximum temperature reached at the canister/buffer interface is about 66 °C, corresponding to a temperature rise of about 54 °C, after about 12 years. The results of the calculations are presented in Figures 1 - 5 (in Appendix I). A perspective plot showing the temperature distribution at the *time = 11.4 years* is presented in Figure 5 (in Appendix I).

As could be observed in Figures 1b, 2b, and 3b the temperature within the canister region equalizes practically instantaneously. This is a

direct consequence of using the "copper like" equivalent canister with its relatively high value of the thermal conductivity.

CBT1b (3.0x30m): This case is a variation of the base case in which the canister spacing was reduced to 3 m. This value was considered the lower tolerance limit to the canister spacing in the present study without considerations of other aspects such as the mechanical strength of the repository that might stipulate a somewhat higher value. This variation increased the maximum temperature at the canister/buffer interface to 94 °C, corresponding to a temperature rise of about 82 °C. The maximum occurred after about 21 years.

SKB 91 Canister - Tunnel spacing=20 m

The following cases were carried out: CBT1d (6.2x20m), CBT1j (5.0x20m), CBT1e (4.2x20m), CBT1h (3.8x20m), CBT1g (3.8x20m) and CBT1c (3.0x20m). The results of the calculations are summarized in Table V.

CBT1d (6.2x20m): This case is a variation of the base case with a canister spacing of 6.2 m and the tunnel spacing reduced to 20 m. The maximum temperature at the canister/buffer interface was about 73 °C. This means that reducing the tunnel spacing from 30 to 20 metres will increase the maximum temperature at the canister/buffer interface with only about 7 °C.

CBT1e (4.2x20m): This case is a variation of the previous case with a reduction of the canister spacing to 4.2 m. The maximum temperature at the canister/buffer interface was about 91 °C after about 34 years.

CBT1h (3.8x20m): This case, with a canister spacing of 3.8m and a tunnel spacing of 20 m, resulted in a maximum temperature of about 99.3 °C (corresponding to a temperature rise of about 87 °C) after about 60 years at the interface between the canister and buffer. From a thermal point of view, this case is considered to represent, the lower tolerance limit of the canister spacing for a tunnel spacing of 20 m.

CBT1c (3.0x20m): This case, with a canister spacing of 3 m and a tunnel spacing of 20 m, was included for the sake of comparison with the base case (CBT1a) with a tunnel spacing of 30 m. The resulting maximum temperature at the canister/buffer interface was about 116 °C, corresponding to a temperature rise of about 104 °C.

PLAN 87 Canister

CBT1f (6.2x30m): This case represents a canister material variation of the base case (CBT1a), in which the present SKB 91 Canister thermal properties have been replaced by the thermal properties used in the previous investigations (Tarandi [1983] and Ageskog [1987]). Thus the specific heat per unit volume $(\rho C)^* = 1.5 \cdot 10^6$ [$MJm^{-3}K^{-1}$] was substituted for $(\rho C)^* = 2.18 \cdot 10^6$ [$MJm^{-3}K^{-1}$] and the thermal conductivity $\lambda_c = 3.0$ [$Wm^{-1}K^{-1}$] was substituted for $\lambda_c = 390$ [$Wm^{-1}K^{-1}$], respectively.

The maximum temperature at the centre of the canister was about 78 °C (corresponding to a temperature increase of about 66 °C) and was reached after about 8 years. The maximum temperature reached at the canister/buffer interface was about 73 °C (corresponding to a temperature increase of about 61 °C) and was reached after about 9 years. It should be pointed out that the temperature maxima reached at the mid-points between the canisters and tunnels, respectively, are about the same as in the base case. Moreover, also the time points of the temperature maxima at the mid-points were about the same as in the base case.

TABLE IV. Summary of the results from the SKB 91 Canister settings with a tunnel spacing equal to 30 metres.

Code	Geometric properties		Peak temperature T_{max} (°C) and time t_{peak} (years)									
			Canister		Buffer		Rock		x = l_x		y = l_y	
	l_x	l_y	T_{max}	t_{peak}	T_{max}	t_{peak}	T_{max}	t_{peak}	T_{max}	t_{peak}	T_{max}	t_{peak}
CBT1a[3]	15	3.1	66.4	11.8	66.4	11.8	50	32	43	469	45	351
(CBT1f[4]	15	3.1	78	8	73	9	51	23	43	427	45	353)
CBT1i	15	2.5	73	13	73	13	57	52	———		———	
CBT1k	15	2.0	81	15	81	15	66	72	———		———	
CBT1b	15	1.5	94	21	94	21	81	270	75	485	81	270

TABLE V. Summary of the results from the SKB 91 Canister settings with a tunnel spacing equal to 20 metres.

Code	Geometric properties		Peak temperature T_{max} (°C) and time t_{peak} (years)									
			Canister		Buffer		Rock		x = l_x		y = l_y	
	l_x	l_y	T_{max}	t_{peak}	T_{max}	t_{peak}	T_{max}	t_{peak}	T_{max}	t_{peak}	T_{max}	t_{peak}
CBT1d	10	3.1	73	18	73	18	62	297	58	472	60	414
CBT1j	10	2.5	83	26	83	26	———		———		———	
CBT1e	10	2.1	91	34	91	34	84	312	80	469	81	391
CBT1h	10	1.9	99	60	99	60	———		———		———	
CBT1g	10	1.8	103	60	103	60	———		———		———	
CBT1c	10	1.5	116	306	116	306	113	352	108	444	112	398

where l_x is half the spacing between tunnels, l_y is half the spacing between the canisters, T_{max} is the maximum temperature and t_{peak} is the time elapsed at the maximum temperature. The inconsistencies of the time points for the long term maxima are due to the fairly large time steps that were used towards the end of each calculation period.

[3] The calculations during the first 40 years were performed with a more refined element mesh (280 elements and 2871 nodes) and an initial time step of $5 \cdot 10^3$ seconds in order to establish more accurately the transient behaviour of the initial period.

[4] Comparative calculation with PLAN 87 Canister thermal properties.

7. CONCLUSIONS

The maximum temperature reached in the base case (30 m tunnel spacing and 6.2 m canister spacing) was about 66 °C (corresponding to a temperature rise of about 54° C) at the canister surface, and about 50 °C (corresponding to a temperature rise of about 38 °C) at the interface between the buffer and the rock.

The results of reducing the tunnel spacing in the base case (6.2 m canister spacing, 30 m tunnel spacing) from 30 to 20 m resulted in an increase of the the maximum temperature at the canister/buffer interface of only about 7 °C (i.e. the maximum temperature at the canister/buffer interface increased from 66 °C to about 73 °C).

Reducing the canister spacing from 6.2 to 3 m, i.e. to the considered minimum canister spacing in the base case, increased the maximum temperature at the canister/buffer interface with about 18 °C. Thus resulting in a temperature maximum at the canister/buffer interface of about 94 °C (corresponding to a temperature rise of about 82 °C).

The considered 100 °C upper tolerance limit of the temperature maximum at the canister/buffer interface was reached for a configuration with a canister spacing of about 3.8 m and a tunnel spacing of 20 m.

A comparative calculation using the "PLAN 87 Canister" thermal properties of the canister region indicates that calculations with the SKB 91 (homogenized "equivalent" copper) Canister lead to about 10 per cent lower temperature maximum at the canister surface than that of the conservative calculations with the "PLAN 87 Canister" thermal properties, as used in the previous investigations.

It should be mentioned that the thermal properties assigned to the canister region has very little influence on the temperature distribution in the "far field" region. In fact the temperature maxima become about the same already at the buffer/rock interface.

8. REFERENCES

1. Ageskog, L., 1987. Personal communication.

2. Ahlbom, K., Tirén, S., 1989,
Overview of geologic and hydrogeologic character of the Finnsjön site and its surroundings, SKB AR 89-08.

3. Bergström, A., 1990, Swedish Nuclear Fuel and Waste Management Co, Box 5864, S-102 48 Stockholm, Sweden, Personal communication.

4. Kjellbert, N., 1990,
"Bränslemängder. Radionuklidinnehåll, Resteffekter och Typkapsel för SKB91", SKB AR 90-41.

5. Tarandi, T., 1983,
"Calculated temperature field in and around a repository for spent nuclear fuel", SKBF-KBS TR 83-22, April 1983, 30 p.

6. Thunvik, R., Braester, C., 1980,
"Hydrothermal conditions around a radioactive waste repository", SKBF-KBS TR 80-19, Dec. 1980, 143 p.

APPENDIX I : Graphical display of the results from the base case

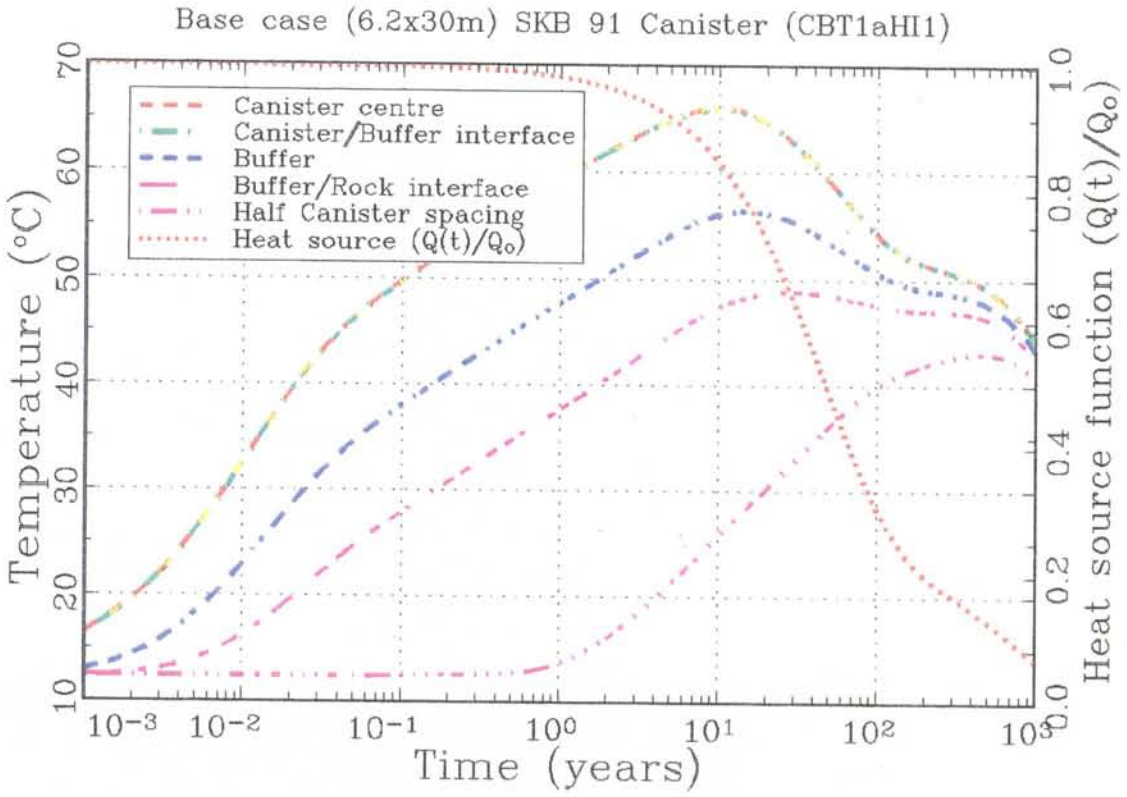

Figure 1a. Results from the base case (CBT1aHI1). Time dependent temperature curves for selected points along a line from the centre of the canister perpendicular to the tunnels. The distance between tunnels = 30 m and the distance between the canisters = 6.2 m.

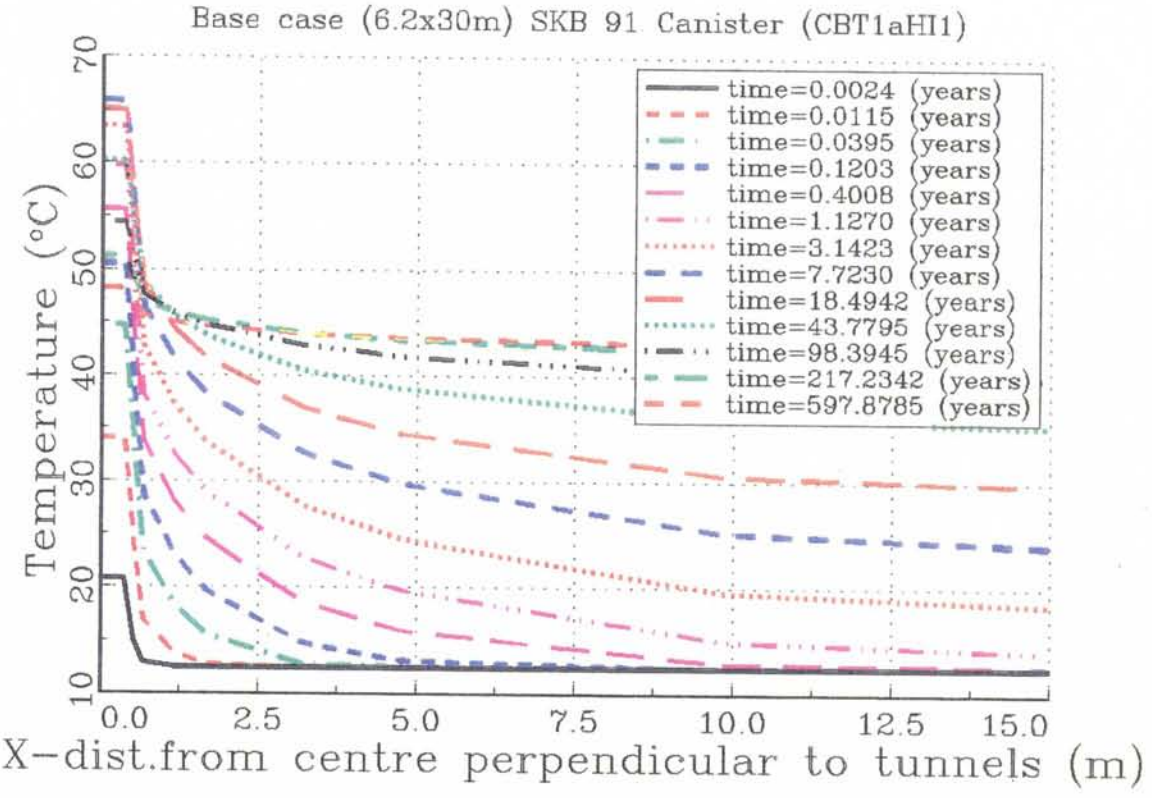

Figure 1b. Results from the base case (CBT1aHI1). Temperature profiles perpendicular to the the tunnel direction: $0 < x < 15$, $y = 0$, $z = 1002.75$. The distance between the tunnels = 30 m and the distance between the canisters = 6.2 m.

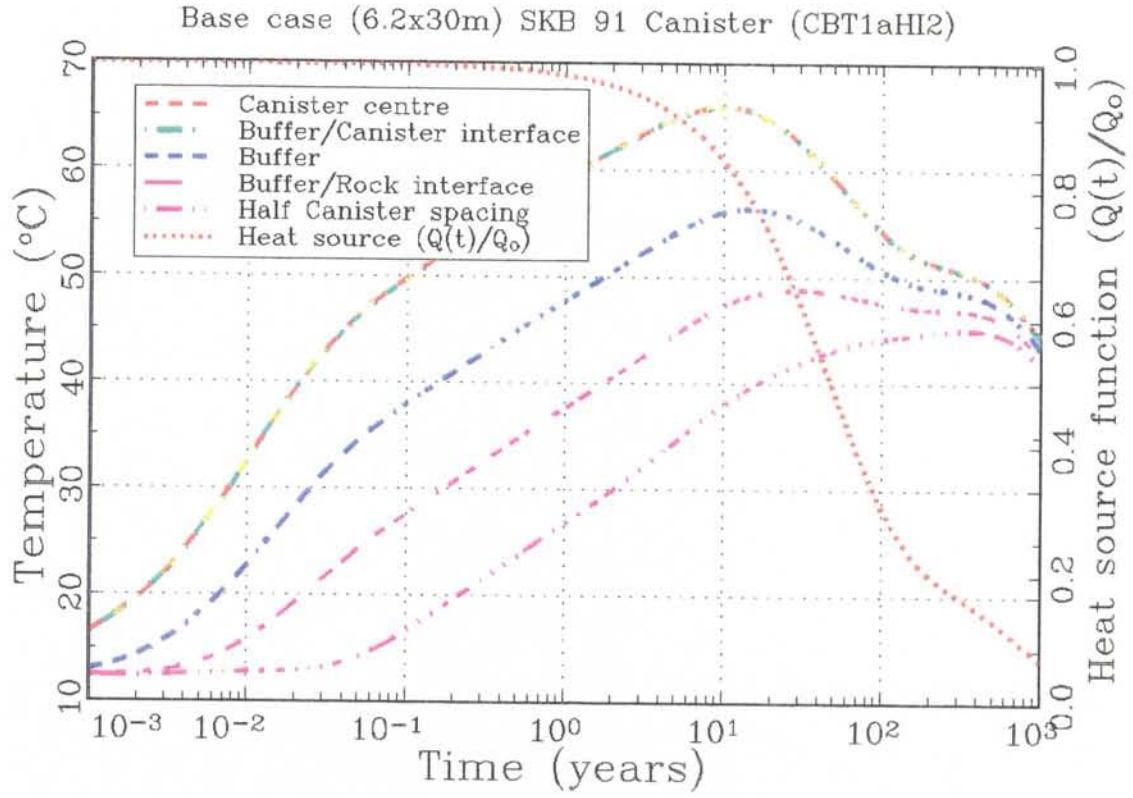

Figure 2a. Results from the base case (CBT1aHI2). Time dependent temperature curves for selected points along a line from the centre of the canister in the direction of the tunnels. The distance between the tunnels = 30 m and the distance between the canisters = 6.2 m.

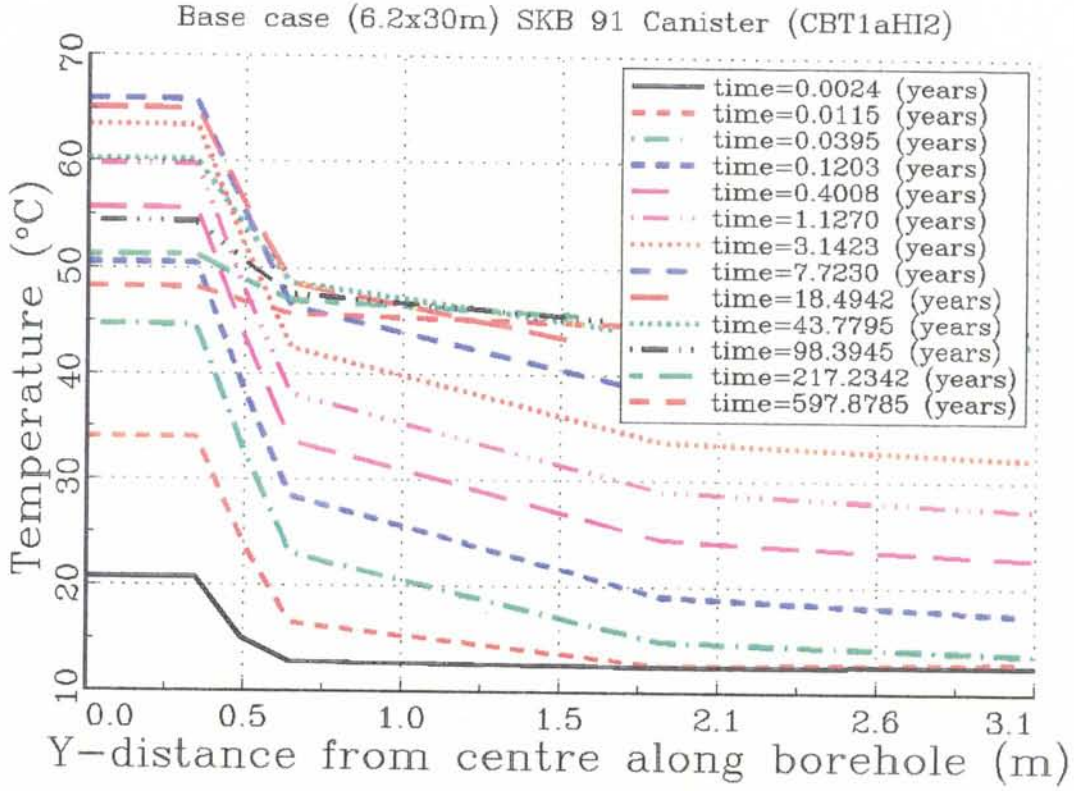

Figure 2b. Results from the base case (CBT1aHI2). Temperature profiles along the tunnel direction: x = 0, 0 < y < 3.1, z = 1002.75. The distance between the tunnels = 30 m and the distance between the canisters = 6.2 m.

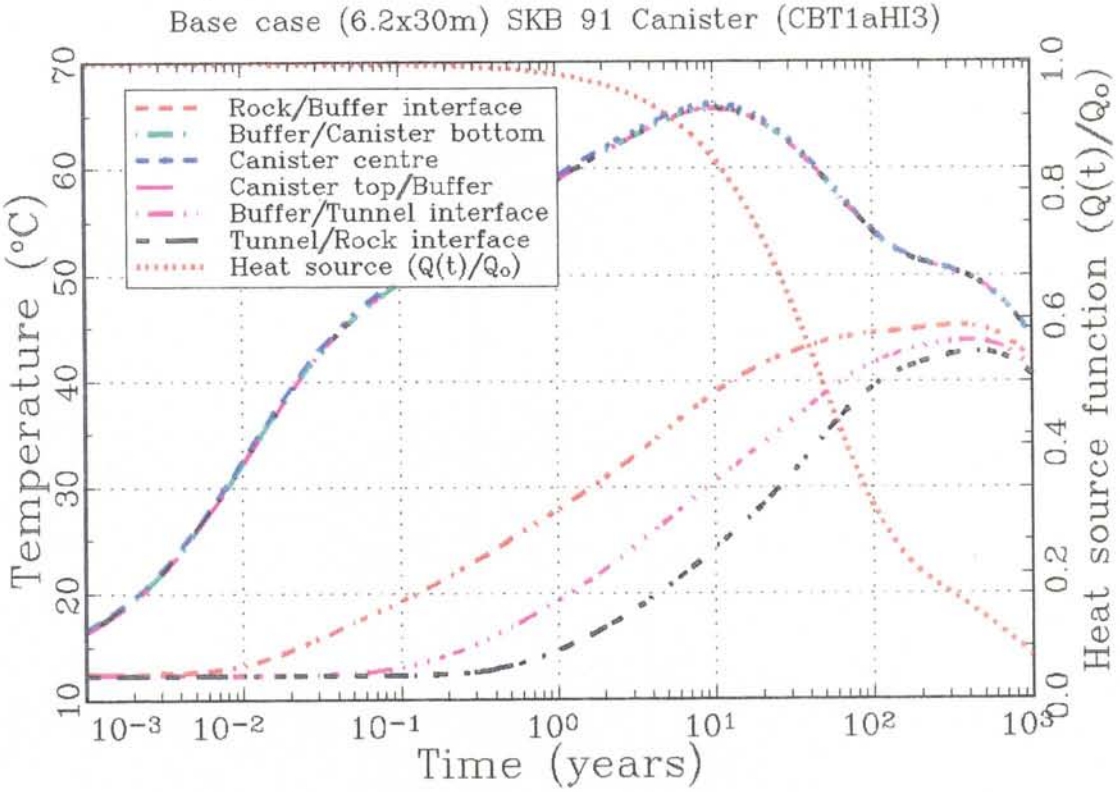

Figure 3a. Results from the base case (CBT1aHI3). Time dependent temperature curves for selected points along the centre line of the borehole. The distance between the tunnels = 30 m and the distance between the canisters = 6.2 m.

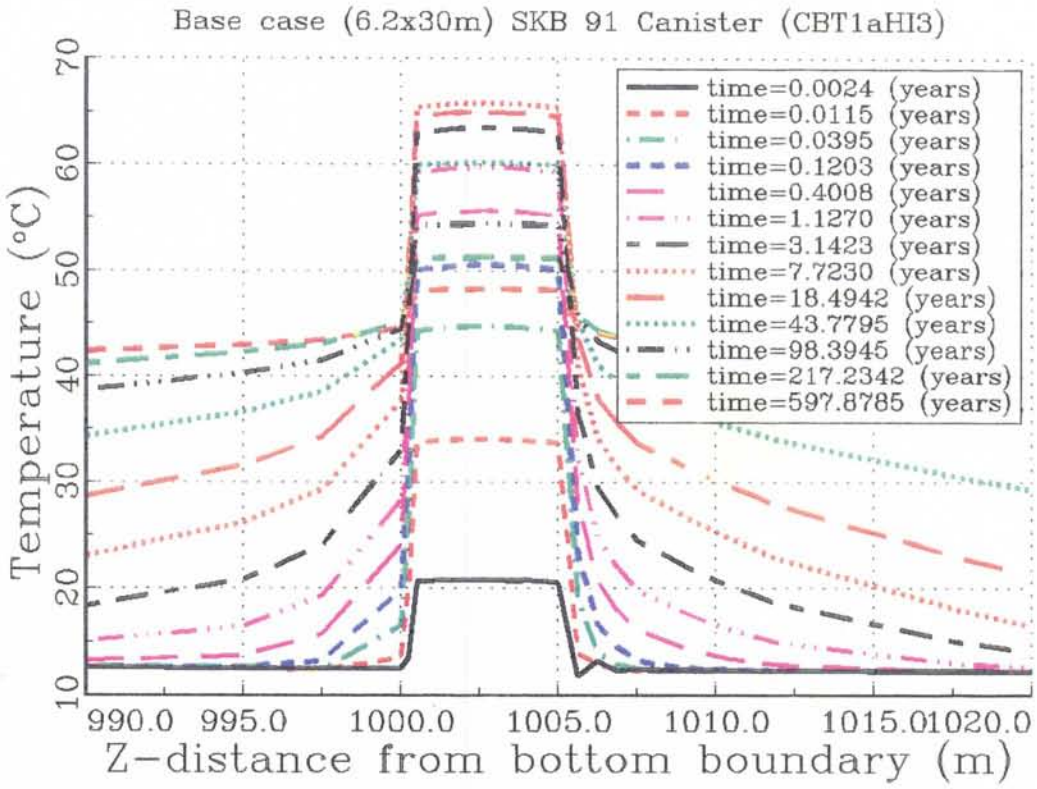

Figure 3b. Results from the base case (CBT1aHI3). Temperature profiles along the centre line of the borehole: x = 0, y = 0, 990 < z < 1020. The distance between the tunnels = 30 m and the distance between the canisters = 6.2 m.

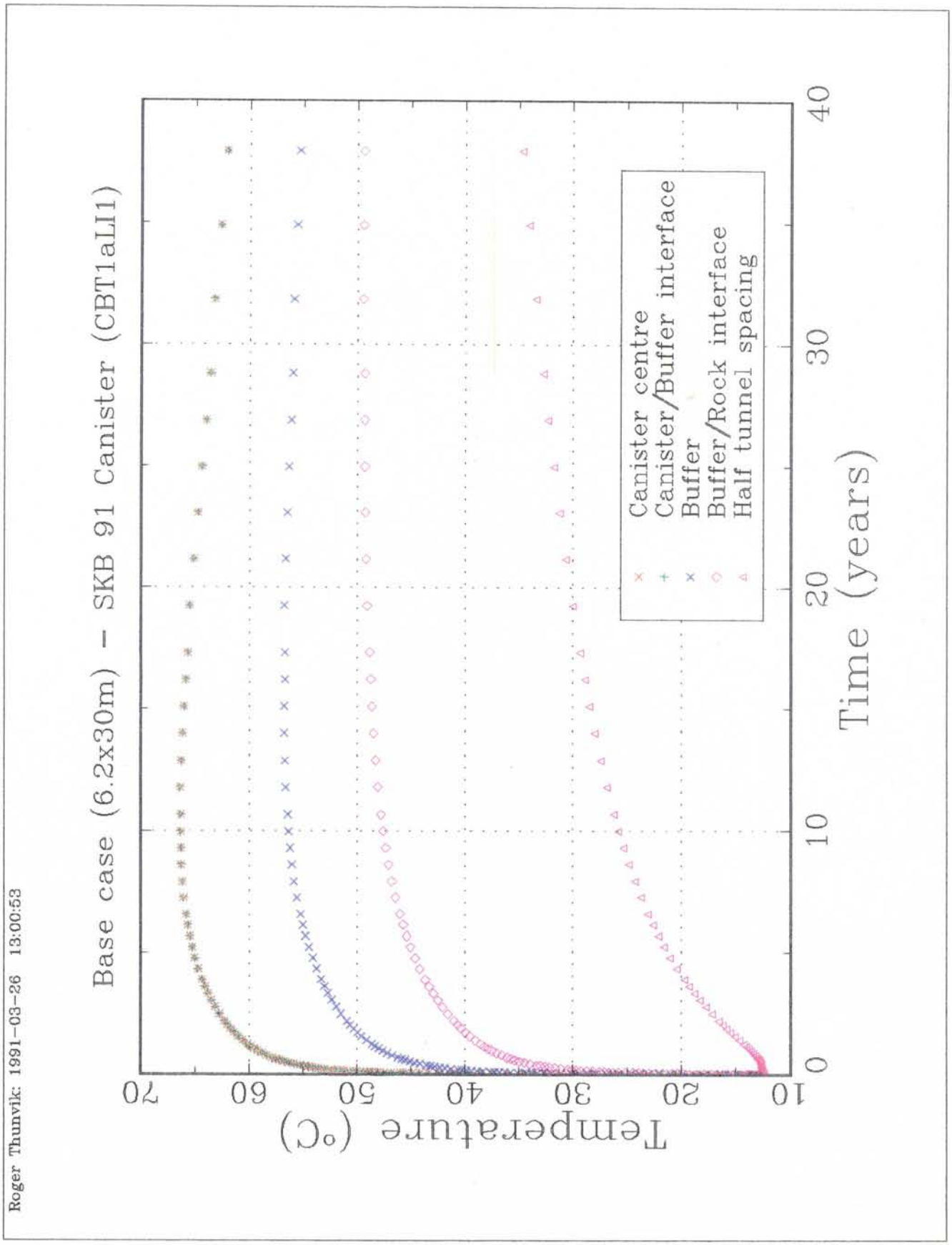

Figure 4. Results from the base case (CBT1aLI1). Time dependent temperature curves during 40 years for selected points along a line from the centre of the canister perpendicular to the tunnels. The distance between tunnels = 30 m and the distance between the canisters = 6.2 m.

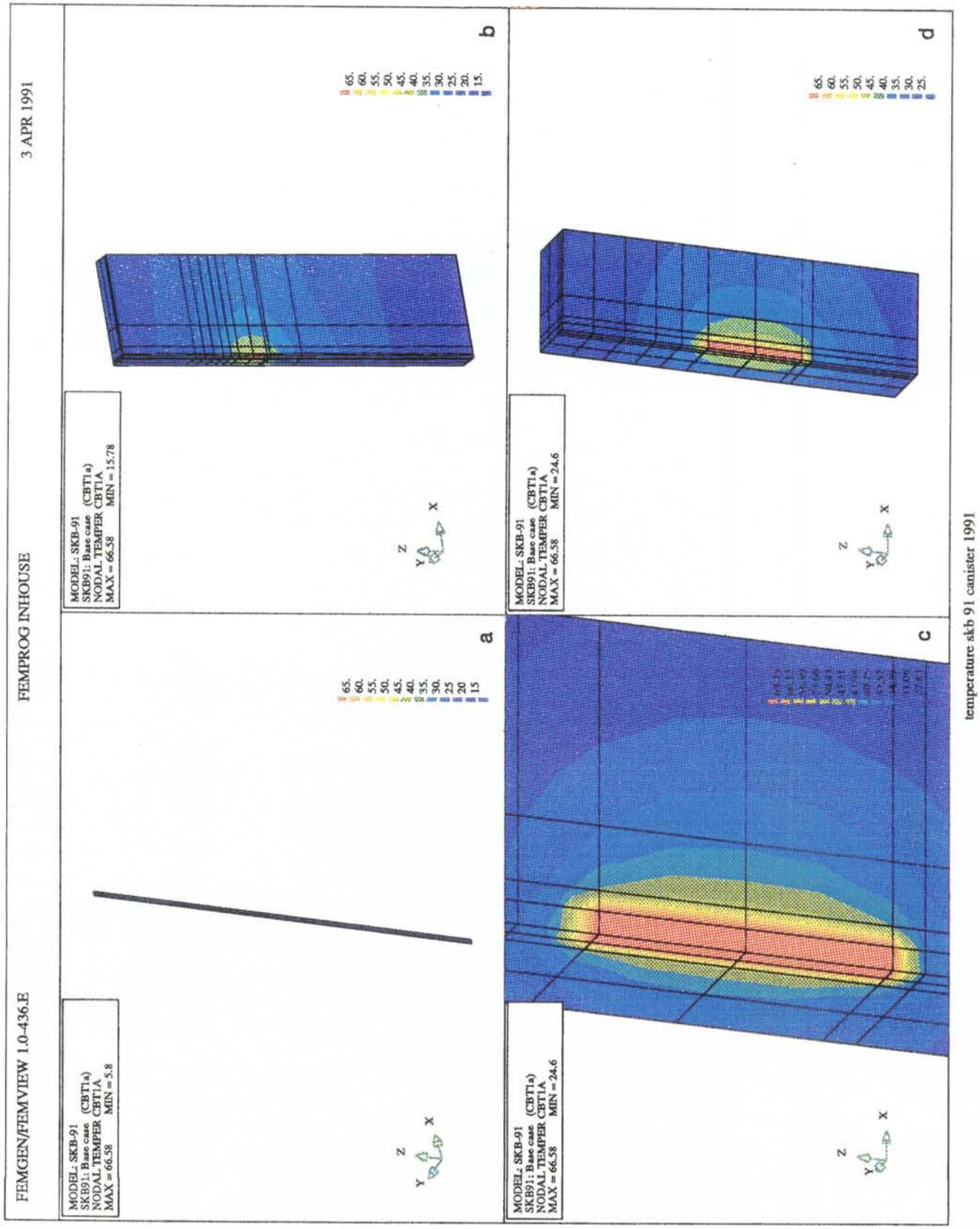

Figure 5. Results from the base case (CBT1a). Perspective plots showing the distribution of the temperature contour lines at the time = 11.4 years: (a) shows the entire flow domain while (b), (c) and (d) show close-ups of the region around the canister.

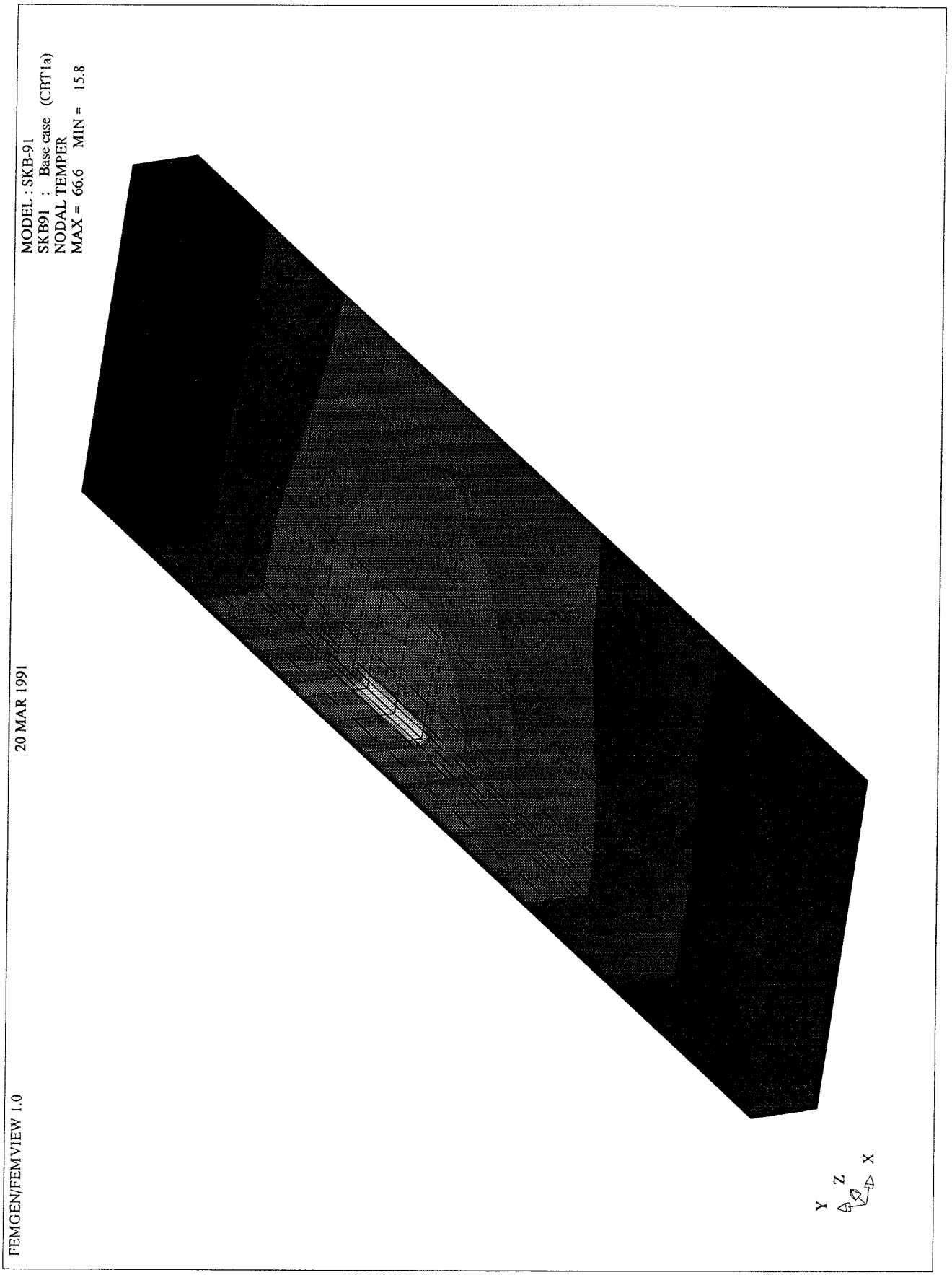

Figure 6 . Results from the base case (CBT1a). Perspective plot showing the distribution of the temperature contour lines around the canister at the time = 11.4 years.

APPENDIX II : Short description of the heat flow model used in the calculations

SHORT DESCRIPTION OF THE FLOW MODEL

Introduction

The finite element method was adopted for solving a set of transient heat flow equations in two or three dimensions for a Cartesian coordinate system or alternatively in two dimensions for an axisymmetric coordinate system.

The flow domain may be discretized into quadrilateral 8- or 9-node elements in two dimensions, or 8-27 node hexahedral elements in three dimensions. The 8-node hexahedron applies to linear interpolation, while the 27-node hexahedron applies to quadratic interpolation over the flow domain.

The thermal properties such as the specific heat and the thermal conductivity may be constant in space (over elements) and time, or varying in time or temperature dependent. In the present calculations all physical properties have been assumed to be constant over each element.

Two types of boundary conditions are considered: (i) Prescribed fixed or time dependent temperature values along a boundary or (ii) Prescribed heat flux across a boundary. The time integration is according to backward Euler, which is an implicit method. The time step scheme is usually pre-specified by the user but an automatic time step selection routine has been implemented. In the latter case the local truncation errors are checked and used for selecting the time steps.

The model program is written in Fortran 77 and implemented on a 386-PC. A graphical interface for the display of the various types of results was written in Microsoft C.

Model equations

Heat conduction is governed by the following equations:
The heat flux equation (Fourier's law)

$$q_i = - \lambda T_{,i} \tag{1}$$

where q_i is the thermal flux in the i direction, λ denotes the thermal conductivity, and T is temperature.

The thermal energy conservation equation

$$(\rho C T)_{,t} + q_{i,i} + Q = 0 \tag{2}$$

Substitution of (1) into (2) yields

$$(\rho C T)_{,t} - (\lambda T_{,i})_{,i} + Q(t) = 0 \tag{3}$$

where ρ the density, C is the specific heat, $T = T(x,y,z)$ is the temperature, λ is the thermal conductivity and $Q(t)$ represents the time dependent heat source.

Boundary and initial conditions

The boundary conditions are

$$\begin{aligned}
&0 < x < l_x \; ; \; 0 < y < l_y \; ; \; z = 0: \quad T = T_{bottom} \\
&0 < x < l_x \; ; \; 0 < y < l_y \; ; \; z = l_z: \; T = T_{surf} \\
&x = 0 \; ; \; 0 < y < l_y \; ; \; 0 < z < l_z: \; q_{,x} = 0 \\
&x = l_x \; ; \; 0 < y < l_y \; ; \; 0 < z < l_z: \; q_{,x} = 0 \\
&y = 0 \; ; \; 0 < x < l_x \; ; \; 0 < z < l_z: \; q_{,y} = 0 \\
&y = l_y \; ; \; 0 < x < l_x \; ; \; 0 < z < l_z: \; q_{,y} = 0
\end{aligned} \tag{4}$$

where l_x, l_y and l_z are the dimensions of the domain in the x, y, and z directions, respectively, and T_{surf} denotes the prescribed temperature on top of the rock surface and T_{bottom} denotes the prescribed temperature on the bottom of the flow domain, respectively.

The initial condition considered is a reference temperature assumed to follow the geothermal gradient. A distributed heat source ($Q(t)$) corresponding to the variation in time of the thermal energy released from the radioactive waste is applied at the canister location.

The heat source

The heat source is applied at

$$0 < x < l_c \ ;$$

$$0 < y < l_c \ ;$$

$$z_{canister} < z < z_{canister} + h : \quad Q = Q\ (t)$$

where $l_c = \frac{\sqrt{\pi}}{2} r_c$, (r_c is the canister radius) is the side of the "equivalent" cross-section square of the canister and h is the height of the canister. The time dependent variation of the heat generation per canister is approximated by a function of the following type:

$$Q(t)/Q_o = \left(\alpha_1 e^{-\alpha_2 t} + (1-\alpha_1) e^{-\alpha_3 t} \right)$$

where Q_o denotes the heat effect at the time of the deposition and α_1, α_2 and α_3 are constant coefficients. These are determined by minimizing a function for the sum of the squares of the differences between the heat function values and the observed values.

In the numerical scheme the time average value of the heat source is used for each time step. Integrating the above function over a time interval ($t^{(n)} \le t \le t^{(n)}+\Delta t$) and dividing by the time step, we obtain

$$(Q(t)/Q_o)^{(n)} = \frac{\alpha_1}{\alpha_2 \Delta t} e^{-\alpha_2 t^{(n)}} \left(1 - e^{-\alpha_2 \Delta t}\right) + \frac{1-\alpha_1}{\alpha_3 \Delta t} e^{-\alpha_3 t^{(n)}} \left(1 - e^{-\alpha_3 \Delta t}\right)$$

where $t^{(n)}$ is current time level and Δt is current time step.

Method of solution

The equations were solved numerically using the Galerkin finite element method. First, the following trial functions are introduced

$$T = \Psi^J \, T^J \tag{5}$$

where $\Psi^J = \Psi^J(x_i)$ represents the basis functions chosen to satisfy the essential boundary conditions.

The same basis functions are also used to express the variation in the material properties over the elements, e.g.,

$$\rho = \Psi^K \, \rho^K \tag{6}$$

Making use of the orthogonality conditions, according to Galerkin's method, we obtain

$$< \rho \, C \, T_{,t} \, , \, \Psi^I > - < (\lambda \, T_{,i})_{,i} \, , \, \Psi^I > + < q^* , \, \Psi^I > = 0 \tag{7}$$

Applying Green's theorem to the second order terms in (7), we obtain

$$< \rho \, C \, T_{,t}, \Psi^I > + < \lambda \, T_{,i}, \Psi^I_{,i} > - \int_\Gamma \lambda \, T_{,i} \Psi^I d\Gamma_i + <q^*, \, \Psi^I> = 0 \tag{8}$$

Substitution of (5) into (8) yields

$$\rho \, C \, T^J \int \Psi^I \Psi^J \, dR + T^J \int \lambda \, \Psi^I \, \Psi^J \, dR$$

$$- \int_\Gamma e^n \, \Psi^I d\Gamma_i + q^{*K} \int \Psi^I \Psi^K dR \; = 0 \tag{9}$$

This equation may be expressed in a matrix form as follows

$$[A]\{T_{,t}\} + [B]\{T\} + [C] = 0 \tag{10}$$

and using a finite difference approximation for the time derivative, we obtain

$$\frac{1}{\Delta t} \, [A] \, (\{T\}^{n+1} - \{T\}^n) + [B]\{T\}^{n+1} + [C] = 0 \tag{11}$$

or

$$\left(\frac{1}{\Delta t} \, [A] + [B] \right) \{T\}^{(n+1)} = \frac{1}{\Delta t} \, [A]\{T\}^{(n)} - [C] \tag{12}$$

where the superscript n denotes the time level.

The algebraic matrix problem (12) is solved using the frontal method.

List of symbols

l_c	equivalent canister side ($l_c = \frac{\sqrt{\pi}}{2}$ r)
C	heat capacity
e^n	normal component of the heat flux at the boundary
h	height of canister
l_x	the length of the investigated domain in the x-direction (= tunnel spacing/2)
l_y	the length of the investigated domain in the y-direction (= canister spacing/2)
l_z	the length of the investigated domain in the z-direction
q	thermal flux
Q	source/sink in the energy conservation equation
Q_o	initial strength of the heat source function
r_c	canister radius
t	time
Δt	time interval
T	temperature
x	Cartesian coordinate in the horizontal plane
y	Cartesian coordinate in the horizontal plane
z	Cartesian coordinate in the vertical direction
t	time

Greek

$\alpha_1, \alpha_2, \alpha_3$	coefficients in the heat source function
λ	thermal conductivity
ρ	density
Ψ	basis function

Subscripts

i,j	indices for Cartesian tensor notation; repeated indices indicate summation over these indices (i,j = 1,2,3)
$,i$	spatial derivative (i = 1,2,3)
$,t$	partial time derivative

Superscripts

I,J,K -	node indices, repeated indices indicate summation over these indices (I,J,K =1,2,...N, where N is the number of nodal points

List of SKB reports

Annual Reports

1977-78
TR 121
KBS Technical Reports 1 – 120
Summaries
Stockholm, May 1979

1979
TR 79-28
The KBS Annual Report 1979
KBS Technical Reports 79-01 – 79-27
Summaries
Stockholm, March 1980

1980
TR 80-26
The KBS Annual Report 1980
KBS Technical Reports 80-01 – 80-25
Summaries
Stockholm, March 1981

1981
TR 81-17
The KBS Annual Report 1981
KBS Technical Reports 81-01 – 81-16
Summaries
Stockholm, April 1982

1982
TR 82-28
The KBS Annual Report 1982
KBS Technical Reports 82-01 – 82-27
Summaries
Stockholm, July 1983

1983
TR 83-77
The KBS Annual Report 1983
KBS Technical Reports 83-01 – 83-76
Summaries
Stockholm, June 1984

1984
TR 85-01
Annual Research and Development Report 1984
Including Summaries of Technical Reports Issued during 1984. (Technical Reports 84-01 – 84-19)
Stockholm, June 1985

1985
TR 85-20
Annual Research and Development Report 1985
Including Summaries of Technical Reports Issued during 1985. (Technical Reports 85-01 – 85-19)
Stockholm, May 1986

1986
TR 86-31
SKB Annual Report 1986
Including Summaries of Technical Reports Issued during 1986
Stockholm, May 1987

1987
TR 87-33
SKB Annual Report 1987
Including Summaries of Technical Reports Issued during 1987
Stockholm, May 1988

1988
TR 88-32
SKB Annual Report 1988
Including Summaries of Technical Reports Issued during 1988
Stockholm, May 1989

1989
TR 89-40
SKB Annual Report 1989
Including Summaries of Technical Reports Issued during 1989
Stockholm, May 1990

1990
TR 90-46
SKB Annual Report 1990
Including Summaries of Technical Reports Issued during 1990
Stockholm, May 1991

Technical Reports

List of SKB Technical Reports 1991

TR 91-01
Description of geological data in SKB's database GEOTAB
Version 2
Stefan Sehlstedt, Tomas Stark
SGAB, Luleå
January 1991

TR 91-02
Description of geophysical data in SKB database GEOTAB
Version 2
Stefan Sehlstedt
SGAB, Luleå
January 1991

TR 91-03
1. The application of PIE techniques to the study of the corrosion of spent oxide fuel in deep-rock ground waters
2. Spent fuel degradation
R S Forsyth
Studsvik Nuclear
January 1991

TR 91-04
Plutonium solubilities
I Puigdomènech[1], J Bruno[2]
[1]Enviromental Services, Studsvik Nuclear, Nyköping, Sweden
[2]MBT Tecnologia Ambiental, CENT, Cerdanyola, Spain
February 1991

TR 91-05
Description of tracer data in the SKB database GEOTAB
SGAB, Luleå
April, 1991

TR 91-06
Description of background data in the SKB database GEOTAB
Version 2
Ebbe Eriksson, Stefan Sehlstedt
SGAB, Luleå
March 1991

TR 91-07
Description of hydrogeological data in the SKB's database GEOTAB
Version 2
Margareta Gerlach (ed.)
Mark Radon Miljö MRM Konsult AB,
Luleå
December 1991

TR 91-08
Overview of geologic and geohydrologic conditions at the Finnsjön site and its surroundings
Kaj Ahlbom[1], Sven Tirén[2]
[1]Conterra AB
[2]Sveriges Geologiska AB
January 1991

TR 91-09
Long term sampling and measuring program. Joint report for 1987, 1988 and 1989. Within the project: Fallout studies in the Gideå and Finnsjö areas after the Chernobyl accident in 1986
Thomas Ittner
SGAB, Uppsala
December 1990

TR 91-10
Sealing of rock joints by induced calcite precipitation. A case study from Bergeforsen hydro power plant
Eva Hakami[1], Anders Ekstav[2], Ulf Qvarfort[2]
[1]Vattenfall HydroPower AB
[2]Golder Geosystem AB
January 1991

TR 91-11
Impact from the disturbed zone on nuclide migration – a radioactive waste repository study
Akke Bengtsson[1], Bertil Grundfelt[1],
Anders Markström[1], Anders Rasmuson[2]
[1]KEMAKTA Konsult AB
[2]Chalmers Institute of Technology
January 1991

TR 91-12
Numerical groundwater flow calculations at the Finnsjön site
Björn Lindbom, Anders Boghammar,
Hans Lindberg, Jan Bjelkås
KEMAKTA Consultants Co, Stockholm
February 1991

TR 91-13
Discrete fracture modelling of the Finnsjön rock mass
Phase 1 feasibility study
J E Geier, C-L Axelsson
Golder Geosystem AB, Uppsala
March 1991

TR 91-14
Channel widths
Kai Palmqvist, Marianne Lindström
BERGAB-Berggeologiska Undersökningar AB
February 1991

TR 91-15
Uraninite alteration in an oxidizing environment and its relevance to the disposal of spent nuclear fuel
Robert Finch, Rodney Ewing
Department of Geology, University of New Mexico
December 1990

TR 91-16
Porosity, sorption and diffusivity data compiled for the SKB 91 study
Fredrik Brandberg, Kristina Skagius
Kemakta Consultants Co, Stockholm
April 1991

TR 91-17
Seismically deformed sediments in the Lansjärv area, Northern Sweden
Robert Lagerbäck
May 1991

TR 91-18
Numerical inversion of Laplace transforms using integration and convergence acceleration
Sven-Åke Gustafson
Rogaland University, Stavanger, Norway
May 1991

TR 91-19
NEAR21 - A near field radionuclide migration code for use with the PROPER package
Sven Norman[1], Nils Kjellbert[2]
[1]Starprog AB
[2]SKB AB
April 1991

TR 91-20
Äspö Hard Rock Laboratory. Overview of the investigations 1986-1990
R Stanfors, M Erlström, I Markström
June 1991

TR 91-21
Äspö Hard Rock Laboratory. Field investigation methodology and instruments used in the pre-investigation phase, 1986-1990
K-E Almén, O Zellman
June 1991

TR 91-22
Äspö Hard Rock Laboratory. Evaluation and conceptual modelling based on the pre-investigations 1986-1990
P Wikberg, G Gustafson, I Rhén, R Stanfors
June 1991

TR 91-23
Äspö Hard Rock Laboratory. Predictions prior to excavation and the process of their validation
Gunnar Gustafson, Magnus Liedholm, Ingvar Rhén, Roy Stanfors, Peter Wikberg
June 1991

TR 91-24
Hydrogeological conditions in the Finnsjön area. Compilation of data and conceptual model
Jan-Erik Andersson, Rune Nordqvist, Göran Nyberg, John Smellie, Sven Tirén
February 1991

TR 91-25
The role of the disturbed rock zone in radioactive waste repository safety and performance assessment. A topical discussion and international overview.
Anders Winberg
June 1991

TR 91-26
Testing of parameter averaging techniques for far-field migration calculations using FARF31 with varying velocity.
Akke Bengtsson[1], Anders Boghammar[1], Bertil Grundfelt[1], Anders Rasmuson[2]
[1]KEMAKTA Consultants Co
[2]Chalmers Institute of Technology

TR 91-27
Verification of HYDRASTAR. A code for stochastic continuum simulation of groundwater flow
Sven Norman
Starprog AB
July 1991

TR 91-28
Radionuclide content in surface and groundwater transformed into breakthrough curves. A Chernobyl fallout study in an forested area in Northern Sweden
Thomas Ittner, Erik Gustafsson, Rune Nordqvist
SGAB, Uppsala
June 1991

TR 91-29
Soil map, area and volume calculations in Orrmyrberget catchment basin at Gideå, Northern Sweden
Thomas Ittner, P-T Tammela, Erik Gustafsson
SGAB, Uppsala
June 1991

TR 91-30
A resistance network model for radionuclide transport into the near field surrounding a repository for nuclear waste (SKB, Near Field Model 91)
Lennart Nilsson, Luis Moreno, Ivars Neretnieks, Leonardo Romero
Department of Chemical Engineering,
Royal Institute of Technology, Stockholm
June 1991

TR 91-31
Near field studies within the SKB 91 project
Hans Widén, Akke Bengtsson, Bertil Grundfelt
Kemakta Consultants AB, Stockholm
June 1991

TR 91-32
SKB/TVO Ice age scenario
Kaj Ahlbom[1], Timo Äikäs[2], Lars O. Ericsson[3]
[1]Conterra AB
[2]Teollisuuden Voima Oy (TVO)
[3]Svensk Kärnbränslehantering AB (SKB)
June 1991

TR 91-33
Transient nuclide release through the bentonite barrier - SKB 91
Akke Bengtsson, Hans Widén
Kemakta Konsult AB
May 1991

TR 91-34
SIMFUEL dissolution studies in granitic groundwater
I Casas[1], A Sandino[2], M S Caceci[1], J Bruno[1], K Ollila[3]
[1]MBT Tecnologia Ambiental, CENT, Cerdanyola, Spain
[2]KTH, Dpt. of Inorganic Chemistry, Stockholm, Sweden
[3]VTT, Tech. Res. Center of Finland, Espoo, Finland
September 1991

TR 91-35
Storage of nuclear waste in long boreholes
Håkan Sandstedt[1], Curt Wichmann[1], Roland Pusch[2], Lennart Börgesson[2], Bengt Lönnerberg[3]
[1]Tyréns
[2]Clay Technology AB
[3]ABB Atom
August 1991

TR 91-36
Tentative outline and siting of a repository for spent nuclear fuel at the Finnsjön site. SKB 91 reference concept
Lars Ageskog, Kjell Sjödin
VBB VIAK
September 1991

TR 91-37
Creep of OFHC and silver copper at simulated final repository canister-service conditions
Pertti Auerkari, Heikki Leinonen, Stefan Sandlin
VTT, Metals Laboratory, Finland
September 1991

TR 91-38
Production methods and costs of oxygen free copper canisters for nuclear waste disposal
Hannu Rajainmäki, Mikko Nieminen, Lenni Laakso
Outokumpu Poricopper Oy, Finland
June 1991

TR 91-39
The reducibility of sulphuric acid and sulphate in aqueous solution (translated from German)
Rolf Grauer
Paul Scherrer Institute, Switzerland
July 1990

TR 91-40
Interaction between geosphere and biosphere in lake sediments
Björn Sundblad, Ignasi Puigdomenech, Lena Mathiasson
December 1990

TR 91-41
Individual doses from radionuclides released to the Baltic coast
Ulla Bergström, Sture Nordlinder
Studsvik AB
May 1991

TR 91-42
Sensitivity analysis of the groundwater flow at the Finnsjön study site
Yung-Bing Bao, Roger Thunvik
Dept. Land and Water Resources,
Royal Institute of Technology, Stockholm, Sweden
September 1991

TR 91-43
SKB - PNC
Development of tunnel radar antennas
Lars Falk
ABEM, Uppsala, Sweden
July 1991

TR 91-44
Fluid and solute transport in a network of channels
Luis Moreno, Ivars Neretnieks
Department of Chemical Engineering,
Royal Institute of Technology, Stockholm, Sweden
September 1991

TR 91-45
The implications of soil acidification on a future HLNW repository.
Part I: The effects of increased weathering, erosion and deforestation
Josefa Nebot, Jordi Bruno
MBT Tecnologìa Ambiental, Cerdanyola, Spain
July 1991

TR 91-46
Some mechanisms which may reduce radiolysis
Ivars Neretnieks, Mostapha Faghihi
Department of Chemical Engineering, Royal Institute of Technology, Stockholm, Sweden
August 1991

TR 91-47
On the interaction of granite with Tc(IV) and Tc(VII) in aqueous solution
Trygve E Eriksen, Daquing Cui
Royal Institute of Technology, Department of Nuclear Chemistry, Stockholm, Sweden
October 1991

TR 91-48
A compartment model for solute transport in the near field of a respository for radioactive waste (Calculations for Pu-239)
Leonardo Romero, Luis Moreno , Ivars Neretnieks
Department of Chemical Engineering, Royal Institute of Technology, Stockholm, Sweden
October 1991

TR 91-49
Description of transport pathways in a KBS-3 type repository
Roland Pusch[1], Ivars Neretnieks[2], Patrik Sellin[3]
[1] Clay Technology AB. Lund
[2] The Royal institue of Techonology Department of Chemical Engineering, Stockholm
[3] Swedisch Nueclear Fuel and Waste Management Co (SKB), Stockholm
December 1991

TR 91-50
Concentrations of particulate matter and humic substances in deep groundwaters and estimated effects on the adsorption and transport of radionuclides
Bert Allard[1], Fred Karlsson[2], Ivars Neretnieks[3]
[1]Department of Water and Environmental Studies, University of Linköping, Sweden
[2]Swedish Nuclear Fuel and Waste Management Company, SKB, Stockholm, Sweden
[3]Department of Chemical Engineering, Royal Institute of Technology, Stockholm, Sweden
November 1991

TR 91-51
Gideå study site. Scope of activities and main results
Kaj Ahlbom[1], Jan-Erik Andersson[2],
Rune Nordqvist[2], Christer Ljunggren[2], Sven Tirén[2],
Clifford Voss[3]
[1]Conterra AB
[2]Geosigma AB
[3]U.S. Geological Survey
October 1991

TR 91-52
Fjällveden study site. Scope of activities and main results
Kaj Ahlbom[1], Jan-Erik Andersson[2],
Rune Nordqvist[2], Christer Ljunggren[2], Sven Tirén[2],
Clifford Voss[3]
[1]Conterra AB
[2]Geosigma AB
[3]U.S. Geological Survey
October 1991

TR 91-53
Impact of a repository on permafrost development during glaciation advance
Per Vallander, Jan Eurenius
VBB VIAK AB
December 1991

TR 91-54

Hydraulic evaluation of the groundwater conditions at Finnsjön. The effects on dilution in a domestic well

C-L Axelsson[1], J Byström[1], Å Eriksson[1],
J Holmén[1], H M Haitjema[2]
[1]Golder Geosystem AB, Uppsala, Sweden
[2]School of Public and Environmental Affairs,
Indiana University, Bloomington, Indiana, USA
September 1991

TR 91-55

Redox capacity of crystalline rocks. Laboratory studies under 100 bar oxygen gas pressure

Veijo Pirhonen, Petteri Pitkänen
Technical Research Center of Finland
December 1991

TR 91-56

Microbes in crystalline bedrock. Assimilation of CO_2 and introduced organic compounds by bacterial populations in groundwater from deep crystalline bedrock at Laxemar and Stripa

Karsten Pedersen, Susanne Ekendahl,
Johanna Arlinger
Department of General and Marine Microbiology,
University of Göteborg, Göteborg, Sweden
December 1991

TR 91-57

The groundwater circulation in the Finnsjö area - the impact of density gradients

Part A: Saline groundwater at the Finnsjö site and its surroundings

Kaj Ahlbom
CONTERRA AB

Part B: A numerical study of the combined effects of salinity gradients, temperature gradients and fracture zones

Urban Svensson
CFE AB

Part C: A three-dimensional numerical model of groundwater flow and salinity distribution in the Finnsjö area

Urban Svensson
CFE AB
November 1991

TR 91-58

Exploratory calculations concerning the influence of glaciation and permafrost on the groundwater flow system, and an initial study of permafrost influence at the Finnsjön site - an SKB 91 study

Björn Lindbom, Anders Boghammar
Kemakta Konsult AB, Stockholm
December 1991

TR 91-59

Proceedings from the Technical Workshop on Near-Field Performance Assessment for High-Level Waste held in Madrid October 15-17, 1990

Patrik Sellin[1], Mick Apted[2], José Gago[3] (editors)
[1]SKB, Stockholm, Sweden
[2]Intera, Denver, USA
[3]ENRESA, Madrid, Spain
December 1991

TR 91-60

Spent fuel corrosion and dissolution

R S Forsyth[1], L O Werme[2]
[1]Studsvik AB, Nyköping, Sweden
[2]Swedish Nuclear Fuel and Waste Management
Co, Stockholm, Sweden
December 1991